S. Andrieux
(ONERA)

E-mail: stephane.andrieux@onera.fr

DOI: 10.12762/2016.AL12-01

Inverse Problems and Experiments: a Fruitful Symbiosis

This paper offers a partial overview of some techniques and results emanating from inverse problems or signal processing with application to the development or enhancement of the exploitation of data obtained by experiments on physical systems pertaining to the aerospace domain. The first part deals with linear problems encountered in various problems of signal processing, whereas the second one addresses two specific image-based identification techniques. Finally, the conclusion strives to identify some future trends.

Introduction: Experiments, Simulation and Inverse Problems

From its very beginning, experiment has been indissolubly related to measurements and instrumentation, but it is only since a few decades ago that numerical processing, simulation and modeling have been deeply incorporated into the field. Symmetrically, the development of computational physics and mathematics in the mid-fifties opened the way to signal processing, and ten years later to addressing what was known as inverse problems (IP) but was studied until the eighties by a very small scientific community only due to a lack of computational power.

Since that period, a continuous development of the "accompaniment" of experiments by computation and modeling has led to new experiments, unprecedented accuracy, and measurements of "hidden" quantities. At the same time, the volume of experimental data has given rise to new capabilities for the identification of physical or geometrical parameters, and also to the emergence of validation procedures for the simulation means. Table 1 illustrates some of the mutual benefits that experiments, simulation and inverse problems have gained by collaborating.

In this paper, a partial overview will be given of some techniques and results emanating from the signal processing theory and the inverse problem community, which have enhanced, made possible or increased the performance level of experiments. Emphasis will also be placed on the notion of *a priori* information in inverse problems, this information being extracted from all of the knowledge accumulated through experiments. First, linear problems arising essentially from signal processing are addressed. Then, two problems coping with image capturing are investigated, since they are considered to be of utmost importance in aeronautical applications: the first deals with Particle Image Velocimetry for fluid flows, and the second one deals with full-field displacement measurement by digital image correlation in mechanics.

Benefits for Experiments gained from Simulation and IP	Benefits for IP and Simulation gained from Experiments
• Regularization, interpolation (super-resolution) and extrapolation of measurements • Extraction of information from highly noisy measured data • Optimization of instrumentation and location of sensors • Access to non-directly measured quantities or unreachable zones • Consideration of uncertainties • Enhancement of NDT-NDE processes and observation instruments • Hybrid experiments	• Definition of new inverse and identification problems from experimental data and procedures • Identification of model parameters, boundary conditions, and internal sources • Forecasting • Enrichment of a priori information • Validation • New NDT- NDE processes and new observation instruments • Hybrid experiments

Table 1 – Cross-fertilization between Experimentation, Simulation and Inverse Problems

Linear problems

Many examples can be found of linear inverse problems arising from experimental instrumentation or, more directly, from the goal aimed at in the investigation of the reality. Most of the examples fall into the field of Image and Signal Processing: signal deconvolution, image restoration, computed tomography, microwave imaging, and fluorescence imaging, as well as adaptive optics [24] and SAR [65] imaging. The general form of linear inverse problems is written as:

$$g = \boldsymbol{H}f + \varepsilon \tag{1}$$

where g is the measured data (output signal, blurred image, etc.), f is the unknown (input signal, original image) $\boldsymbol{H}$ can be called the forward operator (as it appears in the usual "direct problem"), and lastly ε is the noise or the error. Whereas seeking g when the pair $(f, \boldsymbol{H})$ is given is a direct or forward problem, seeking f with given $(g, \boldsymbol{H})$ is called the estimation or inverse problem, and seeking $\boldsymbol{H}$ (or parameters describing it) with given (f, g) is the identification problem.

As an example, in the deconvolution problem, $\boldsymbol{H}$ is a convolution with kernel h:

$$\boldsymbol{H}(f) = \int h(t-\tau) f(\tau) d\tau \tag{2}$$

$\boldsymbol{H}$ involves the impulse response of an instrument (called point spread function (PSF) in imaging, it is the spatial domain version of the imaging system transfer function). When the PSF is totally unknown one speaks of blind deconvolution, whereas when some measurements or estimations of the PSF are available (but the PSF is not fully known), we have the myopic deconvolution problem, in which both the object and the PSF have to be restored [51].

The operator $\boldsymbol{H}$ generally arises from the modeling of the underlying physics, and can sometimes be a matter of design, like in radar where the $\boldsymbol{H}$ operator is designated as the sensing operator. Note that the general form (1) also encompasses the Bayesian inference approach ([17], [18], [47]) where the pdf of the signal is now the unknown.

Once discretized (or sometimes directly resulting from the physics), $\boldsymbol{H}$ is a (rectangular) matrix, a Toeplitz matrix for deconvolution for example, and (f, g) will be vectors of respective lengths N and M (where generally $N>M$).

Ill-posedness and regularization

Inverse problems are generically ill-posed. From the continuous viewpoint, the ill-posedness arises either from the non-existence of a solution, the non-(finite) uniqueness of the solution or the non-continuity of the solution with respect to the data ([33], [44]). Box 1 gives some details about the ill-posedness of the Fredholm integral equation of the first kind, frequently arising in inverse problems. In the finite dimensional context, these concepts move to a non-invertible (or rectangular with $N>M$) matrix $\boldsymbol{H}$, and severe bad conditioning.

In order to deal with this difficulty, the general procedure is regularization, which was introduced in the sixties ([53], [63]); that is, loosely speaking, accepting to modify the operator or the model in such a way that well-posedness is recovered. The price to pay is a loss of accuracy.

Basically, regularization is performed on a variational form of the inverse problem, in which f is sought as the minimum of a functional (usually chosen as a norm of the gap with respect to the measured data):

$$f = \underset{p}{ArgMin}\, J(p) \tag{3}$$

The regularization is achieved by adding a stabilizing functional $S(p)$ with a (small) scalar regularization parameter α, which is a compromise parameter between the fidelity to the data and the desired properties of the function f that are enforced via the stabilizing functional.

$$J_\alpha(p) = J(p) + \alpha S(p) \tag{4}$$

Again, the choice of the stabilizing functional relies on *a priori* knowledge about the underlying physics. Usual choices for S are either based on regularity requirements on f, or guided by the vicinity of a given value f_0 of f. Historically, the stabilizing functional was the quadratic norm of the gradient of f, in order to smooth out the spatial or temporal oscillations of the signal frequently encountered in ill-posed problems, where the noise in the data is dramatically amplified in the solution. However, since this turns out to be too smoothing, and especially for edge-preserving applications, the total variation regularization or L1 stabilizing functional are used ([21], [54]), or even more sophisticated L1-L2 functionals: quadratic for small gradients and linear for large ones ([14],[23]).

Box 1 – Ill-posedness of the Fredholm integral of first kind

The equation is a typical example of an ill-posed problem and appears in numerous inverse problems:

$$g(x) = \int_J h(x,y) f(y) dy, x \in I$$

The Hadamard ill-posedness occurs under the following situations [3]:

- When the kernel h is continuous, g will be continuous for any measurable function f, therefore, no reasonable function f exists if g exhibits discontinuities,
- If the sign of the kernel is not constant, a non-finite set of solutions can exist. Simply by assuming that $I=J=[0, \pi]$, $h(x,y)=x \sin y$, $g(x)=x$, it is easy to verify that the set $\left\{ f_n(y) = \frac{1}{2} + \sin ny, n \in \mathbb{N} \right\}$ is a family of solutions,
- Thanks to the Lebesgue lemma (if $p(y)$ is continuous, then $\int_0^\pi p(y) \sin nydy \to 0$ when n tends to infinity), the perturbation of the solution can be set to be arbitrarily large whatever the norm of the data perturbation, so no continuity with respect to the data can be achieved.

Although the choice of the regularization parameter is often made on the basis of trial and error procedures, it can also rely on supplementary information about the measurement errors. The discrepancy principles ([10], [50]), for example, propose roughly speaking to determine the parameter α just by choosing the smallest value that makes the fidelity term of the functional be of the same order of magnitude as that of the measurement error: that is, not requiring more fidelity than the error level for the data. A last call to experience for the solution of inverse problems can be the choice of the minimization algorithm starting point, usually called the initial guess.

However, the most striking example of the use of *a priori* information in solving inverse problems is the Bayesian inference approach, where the philosophy is to consider the experiment as a means for adapting the *a priori* knowledge that we have about the situation at hand. More precisely, the Bayes theorem is used to build the posterior probability distribution of the parameters, given the prior distribution and the result of the experiment. In the linear case, the formulation obtained is very similar to the deterministic regularized least-square formulation (Gaussian prior corresponding to the weighted L2 fidelity norm, and the Laplacean prior to L1) with the noticeable difference being that there is no regularization parameter *per se*. The balance between the corresponding fidelity term and regularization term is provided naturally, given by the covariance matrices.

An additional benefit of the probabilistic approaches is that the question of the model used for extracting information or parameters out of the measured data can be addressed. Indeed, using models leads inevitably in an approximation or a systematic error, and to quoting G. Box [15]: "*The most that can be expected from any model is that it can supply a useful approximation to reality: All models are wrong; some models are useful*". This is the reason why some authors plead for the incorporation of uncertainties (and thus for a probabilistic, generally Bayesian, approach [39]): *A model that is wrong can only be useful if we acknowledge the fact that it is wrong […] model discrepancy is an important part of uncertainty quantification and must not be ignored, even though it may be hard to account for* [17].

Compressed sensing

Modeling and using a priori information also play a prominent role in the recent approach of compressed sensing [19]. One of its salient features is the identification of an orthonormal basis, say $\{\Psi_i\}$, where the unknown f has a S-sparse expansion, that is, a low number S of non-zero (or significant) components:

$$f = \sum_{i=1}^{S} f_i \psi_i \qquad S \text{ "small"} \tag{5}$$

The second fundamental premise of compressed sensing is incoherence, because it enables the possibility of performing the determination of f_i with very few samples of the data g. More precisely, if the basis for "representation" of the data g is denoted by $\{\varphi_i\}$, the coherence in IR^n between the "sensing" basis $\{\Psi_i\}$ and the representation basis $\{\varphi_i\}$, is

$$\mu(\varphi,\psi) = \sqrt{n} \max_{1\le i,j\le n} \left|\varphi_i.\psi_j\right| \tag{6}$$

A lower value of μ (note that $1 \le \mu \le \sqrt{n}$) corresponds to a lower correlation between any two elements of each basis [28]. Classical examples of pairs with low coherence are the *Fourier basis-Spikes basis* ($\mu = 1$), which represents maximal incoherence, or the *Noiselets basis-Haar wavelets basis* ($\mu = \sqrt{2}$). Coherence is involved in a quite strong result stating that the number of data sufficient for a good identification of f can be significantly lower than the Nyquist rate given by the Shannon theory: for an IR^n f signal that is S-sparse in the basis $\{\Psi_i\}$ and a set of m measurements selected in the basis uniformly at random, then

$$m \ge C\mu^2 S \log n \quad \Rightarrow \quad \{f^*\}_{i\le S} \text{ is exact} \tag{7}$$

where f^* is the solution of the following l_1 minimization problem, constrained by the m measurements of (1):

$$\min_{\{f\}\in IR^n} \left|\{f\}\right|_1 \quad \text{subject to } g_i = <\boldsymbol{H}f, \varphi_i> \; i = 1,\ldots,m \tag{8}$$

the result (6) being true within an "overwhelming probability" [19]. It is readily seen that for a coherence equal to one, the number m of needed data is of the order $S \log n$. If we now turn to noisy data, the question of robustness with respect to noise becomes central. The version of (8) is now a relaxed version, known as the LASSO or l_1-l_2 regularization ([29], [62], [51], [24], [27], [67]), where advantage is taken of the knowledge of the noise level ε:

$$\min_{\{f\}\in IR^n} \left|\{f\}\right|_1 \text{ subject to } \left\|g - \boldsymbol{H}f\right\|_2 < \varepsilon \tag{9}$$

Using the concept of the isometry constant δ_S for the matrix $\boldsymbol{H}$ and any integer S defined by the smallest number such that:

$$1 - \delta_S \le \frac{\left\|\boldsymbol{H}x\right\|_2^2}{\left\|x\right\|_2^2} \le 1 + \delta_S \quad \forall\, S - sparse\ x \tag{10}$$

[20] showed that the solution f^* of (8) has the following error inequality, when $\delta_{2S} < \sqrt{2} - 1$:

$$\left\|f^* - f\right\|_2 \le \frac{C_0}{\sqrt{S}} \left\|f - f_S\right\|_1 + C_1\varepsilon \tag{11}$$

This means that the error in the reconstruction is just supplemented, in the case of noise, with a term directly proportional to the noise level. Furthermore, [20] claims that the constants C_0 and C_1 are "small" (typically, for $\delta_{2S} = ¼$, C_0 and $C_1 < 6$).

Sparsity can also be enforced within the Bayesian approach to linear inverse problems [47], and also has a wide field of application in the identification of 3D vector fields ([25], [48]).

Completion and interpolation of velocity fields obtained by PIV

According to [64], "*The great challenges of flow dynamics require the validation of physical models with relevant length ranges spanning dozens of orders of magnitude, from a few Angstroms, at which atoms and molecules collide and bond (particularly in combustion), to a meter range (the size of a combustion chamber or a wing). Optical diagnostics are ideal for addressing this enormous challenge as they can span these different scales, offering both a global view through imaging and a microscopic view through spectroscopy. Moreover, these techniques are non-intrusive, so that they do not disturb the system or bias the measurements as other probing techniques do.*"

Unlike Particle Tracking Velocimetry [2], dealing with low seeding density and sparse estimation of the displacement, PIV is based either on direct correlation techniques between two successive images (including fast algorithms on GPUs, like the iterative Lucas-Kanade optical flow algorithm FOLKI [22]), or on image correlation techniques using the optic flow conservation equation. This last equation just expresses the fact that, under the assumption of conservation of the luminance of the particles, the image (gray level) $I(x,t)$ is only transformed by the velocity flow $\boldsymbol{v}$ between two time instants:

$$\partial_t I + \boldsymbol{v}.\nabla I = 0 \tag{12}$$

It is clear that this equation only gives access to limited information about the velocity field, namely the component of $\boldsymbol{v}$ parallel to the gradient of the function I; $\boldsymbol{v}^{\perp}$ remains undetermined (note in passing that no information is gained from a part of the flow with a uniform gray level in the image):

$$\boldsymbol{v} = -\partial_t I \frac{\nabla I}{\|\nabla I\|} + \boldsymbol{v}^{\perp} \ , \ \boldsymbol{v}^{\perp}.\nabla I = 0 \tag{13}$$

Thus, a naïve least-square formulation like the following, striving to minimize the residual of the equation (12), is doomed to fail.

$$\boldsymbol{v}^{opt} = \underset{\boldsymbol{v}}{ArgMin}\, J(\boldsymbol{v}) \equiv \int_{\Omega_m} \left(\partial_t I + \boldsymbol{v}.\nabla I\right)^2 dV \tag{14}$$

For two dimensional domains Ω, [59] showed that regularized functionals consisting of two terms (the first measuring the closeness to the data and the second measuring desired smoothing properties of the solution):

$$J_\alpha(\boldsymbol{v}) = \int_\Omega \left(\partial_t I + \boldsymbol{v}.\nabla I\right)^2 dV + \alpha \int_\Omega \|\nabla \boldsymbol{v}\|^2 dV \tag{15}$$

or

$$\begin{aligned} J_\alpha(\boldsymbol{v}) &= \int_\Omega \left(\partial_t I + \boldsymbol{v}.\nabla I\right)^2 dV + \alpha \int_\Omega \|\nabla \boldsymbol{v}\|^2_{W_I} dV \\ \|\nabla \boldsymbol{v}\|^2_{W_I} &= \nabla v_1.W_I.\nabla v_1 + v_2.W_I.\nabla v_2\ , W_I \\ &= \frac{1}{|\nabla I|^2 + 2\gamma}\left[\nabla I^{\perp} \otimes \nabla I^{\perp} + \gamma Id_2\right], \nabla I^{\perp} \\ &= e_3 \wedge \nabla I \end{aligned} \tag{16}$$

are $H^1(\Omega)$-elliptic (hence convex) for $\alpha > 0$ and have a unique minimizer, which depends continuously on the data. The second regularized functional appears to be more physically grounded (since it turns out that it actually regularizes only the vector field component in the direction parallel to the intensity I, a component which is loosely controlled by the optical flow equation). Nevertheless, the first order Euler conditions for stationarity involve far more complicated boundary conditions for the solution field than for the first functional.

Estimates of fluid flow velocity fields are often corrupted, however, due to various deficiencies of the imaging process, making the physical interpretation of the measurements questionable. Some authors have proposed to deal with vector field estimates from any method and return a "physically plausible denoised version" thereof [66], whereas some more physical considerations can be introduced in the regularization added functional ([36] and the review paper [37]). By designing variational PIV methods, [55] showed how physically consistent flows should be estimated from PIV image sequences utilizing a distributed-parameter control approach. This has been extended in ([56], [57]) to a dynamic setting based on the vorticity transport equation formulation of the Navier-Stokes equation. [68] proposed to achieve spatial and temporal super-resolution of a measured flow. Applications are numerous in aerodynamics, for example in [26] for the analysis of turbulent jets, or for the interaction between shocks and boundary layer, [58].

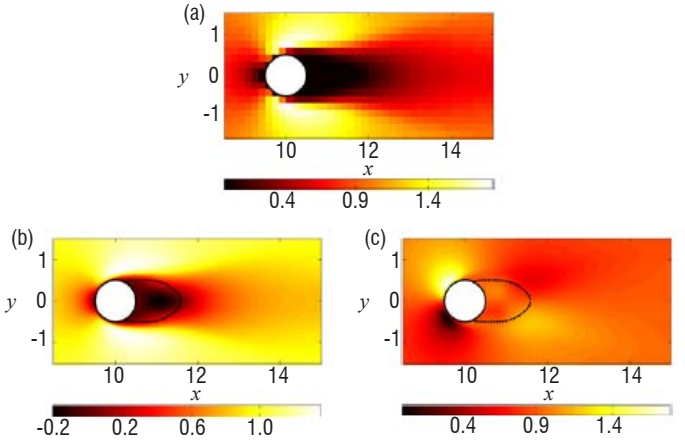

Figure 1 – Reynolds-averaged Navier-Stokes-driven mean-flow reconstruction around a cylinder: *(a)* velocity magnitude measurements, *(b)* and *(c)* reconstructed components of the mean velocity field (from [31])

Apart from the question of noise, which cannot be avoided, one can also be interested in extending the identification of the velocity field within the flow away from a "measurement box" or "measurement slice" Ω_m and in identifying other parameters describing the flow, or involved in its modeling. Two approaches can be proposed, sometimes sharing the final form of the algorithms, but with a different reasoning behind them: the optimal control approach [46] and the data assimilation approach [45]. Figure 1 describes the kind of results that can be achieved.

An optimal control approach for a model problem

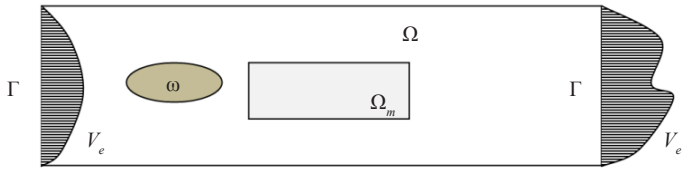

Figure 2 – Sketch of the geometry of the flow data regularization/extension problem

Let Ω be the total volume (or surface) where the velocity field v has to be identified, and let Ω_m be the subdomain where the velocity measurement is made. The inflow and outflow boundaries are denoted by Γ and let us denote the obstacle around which the flow is studied by ω (Figure 2).
In order to then enhance the velocity identification or estimation $\boldsymbol{v}$, and to extend the estimation outside of Ω_m, the following functional is built involving two auxiliary fields as control variables: a volume force density $\boldsymbol{f}$ in Ω and a surface velocity field g on Γ

$$F(\boldsymbol{f}, \boldsymbol{g}) \equiv H\left(\boldsymbol{v}(\boldsymbol{f}, \boldsymbol{g}), \boldsymbol{f}, \boldsymbol{g}\right) \tag{17}$$

with the velocity field $\boldsymbol{v}$ over the entire domain $\Omega\backslash\omega$ being related to the pair $(\boldsymbol{f}, \boldsymbol{g})$ by a state equation $E(\boldsymbol{v}, \boldsymbol{f}, \boldsymbol{g}) = 0$; for example, considering the simplest one:

$$\begin{cases} -\nu\Delta \boldsymbol{v} = \boldsymbol{f}\ in\,\Omega \\ \boldsymbol{v}\big|_{\Gamma} = \boldsymbol{V}^{e} + \boldsymbol{g} \\ \boldsymbol{v}\big|_{\partial\Omega\setminus\Gamma\cup\partial\omega} = 0 \end{cases} \tag{18}$$

This can be viewed as the Stokes equation without the incompressibility constraint div $\boldsymbol{v}=0$, which can hardly be fulfilled in a 2D setting where particles can exhibit a significant out-of-plane velocity component. $\boldsymbol{V}^{e}$ is an estimation of the inflow and outflow condition. The recovery algorithm is then:

$$\begin{aligned} (\boldsymbol{f}^{opt}, \boldsymbol{g}^{opt}) &= Arg\ Min\ F(\boldsymbol{f}, \boldsymbol{g}) \\ \text{and } \boldsymbol{v}^{opt} &= \boldsymbol{v}(\boldsymbol{f}^{opt}, \boldsymbol{g}^{opt}) \end{aligned} \tag{19}$$

where the velocity field $\boldsymbol{v}^{opt}$ is computed through the state equation with the optimal values of the forcing terms. The functional $F_i = H_i + S$ contains two terms. The first (fidelity term) can be the usual optical flow conservation residual, sometimes called the brightness change contrast equation, involving the intensity $I(\boldsymbol{x},t)$ (particle image):

$$H_1(\boldsymbol{v}) = \int_{\Omega_m} \left(\partial_t I + \boldsymbol{v}.\nabla I\right)^2 dV \tag{20}$$

if one deals directly with the analyzed image sequences, or a least-square error over the measured area:

$$H_2(\boldsymbol{v}) = \int_{\Omega_m} \left(\boldsymbol{v} - \boldsymbol{v}_m\right)^2 dV \tag{21}$$

if one deals with a first (rough) identified velocity field $\boldsymbol{v}_m$. The second term is a regularization (and bringing convexity) term, involving the stabilization of semi-norms on the control variables $\boldsymbol{f}$ and $\boldsymbol{g}$:

$$S_{\alpha\beta}(\boldsymbol{v}) = \alpha \|\boldsymbol{f}\|_{\Omega}^2 + \beta \|\boldsymbol{g}\|_{\Gamma}^2 \tag{22}$$

where (α, β) is a pair of (small) positive scalar parameters of the method. Whereas the semi-norm for the regularization of the velocity $\boldsymbol{g}$ can involve its tangential gradient $\nabla_s \boldsymbol{g}$ on Γ (in order to control more the spatial variation of the inlet and outlet velocities rather than their amplitude), the standard L^2 norm should be preferred for the regularization of the source term $\boldsymbol{f}$, as it stands for all of the irregular terms in the Navier-Stokes equation in the state equation.

Let us make a few remarks related to this formulation of the identification problem. First, the state equation is chosen in such a way that, given a pair of (regular) functions $(\boldsymbol{f}, \boldsymbol{g})$, a unique velocity field $\boldsymbol{v}(\boldsymbol{f}, \boldsymbol{g})$ is solution of the equation (18), thanks to the coerciveness of the Laplace operator and to the Lax-Milgram theorem. Second, the regularization term is essential in order to select a solution $\boldsymbol{v}$, just because the degree of freedom inserted in the formulation by the introduction of the unknown pair $(\boldsymbol{f}, \boldsymbol{g})$ is very large. Indeed, one can easily convince oneself that given a pair $(\boldsymbol{f}_0, \boldsymbol{g}_0)$, and accordingly a velocity field $\boldsymbol{v}_0$ solution of the state equation, the following family of triplets $(\boldsymbol{f}+\Delta\boldsymbol{\varphi}, \boldsymbol{g}, \boldsymbol{v}+\boldsymbol{\varphi})$ satisfies the state equation and leads to the same values of the functionals H_i (i=1or 2) for every regular $\boldsymbol{\varphi}$ with compact support in $\Omega\setminus(\Omega_m \cup \omega)$ .The reason why is simply that for every $\boldsymbol{v}$ in the family: $\boldsymbol{v} \equiv \boldsymbol{v}_0$ in Ω_m. Thus, for $\alpha = \beta = 0$, the convex functionals F_i cannot be strictly convex.

On the contrary, for $\alpha, \beta > 0$, the functionals F_i are strictly convex and positive, hence they have a unique minimum (depending on the pair (α,β)). Thus, the regularized identification problem has a unique solution. It is readily seen, thirdly, that the functionals F_i are quadratic (as $\boldsymbol{v}(\boldsymbol{f}, \boldsymbol{g})$ has an affine dependence on $(\boldsymbol{f}, \boldsymbol{g})$). Nevertheless, the implicit dependence of $\boldsymbol{v}$ on $(\boldsymbol{f}, \boldsymbol{g})$) prevents any use of the first order Euler condition for determining the minimum. The solution method is then the direct minimization and, due to the ill-posedness of the problem and to the cost of the computation of the functional F for a given pair $(\boldsymbol{f}, \boldsymbol{g})$, it is essential to have a precise computation of its gradient. The more efficient way to compute it and to take into account the implicit dependence of F with respect to $(\boldsymbol{f}, \boldsymbol{g})$, is the adjoint field approach. This can be achieved by using the following Lagrangian, involving two Lagrange multipliers $(\boldsymbol{w}, \boldsymbol{\mu})$:

$$\begin{aligned} L(\boldsymbol{v}, \boldsymbol{w}, \boldsymbol{\mu}; \boldsymbol{f}, \boldsymbol{g}) = H(\boldsymbol{v}, \boldsymbol{f}, \boldsymbol{g}) - \int_{\Omega} \nu\nabla\boldsymbol{v}.\nabla\boldsymbol{w} dV + \\ \int_{\Omega} \boldsymbol{f}.\boldsymbol{w}\, dV + \int_{\Gamma} \boldsymbol{\mu}.(\boldsymbol{v} - \boldsymbol{V}^{p} - \boldsymbol{g}) dS \end{aligned} \tag{23}$$

The equation for the adjoint field $\boldsymbol{w}$ is obtained by stationarity of the Lagrangian with respect to $\boldsymbol{v}$, and is written as:

$$\begin{cases} -\nu\Delta\boldsymbol{w} = H'_{v}\left(\boldsymbol{v}(\boldsymbol{f}, \boldsymbol{g}), \boldsymbol{f}, \boldsymbol{g}\right)\ in\,\Omega \\ \nu\nabla\boldsymbol{w}.\boldsymbol{n}\big|_{\Gamma} = -\nu\nabla\boldsymbol{v}(\boldsymbol{f}, \boldsymbol{g}).\boldsymbol{n}\big|_{\Gamma} \\ \boldsymbol{w}\big|_{\partial\Omega\setminus\Gamma} = 0 \end{cases} \tag{24}$$

where H'_{v} is the partial derivative of the H functional with respect to $\boldsymbol{v}$; that is, for the two possible choices described previously:

$$\begin{aligned} H'_{v}\left(\boldsymbol{v}(\boldsymbol{f}, \boldsymbol{g}), \boldsymbol{f}, \boldsymbol{g}\right) &= 2\left(\partial_t I + \boldsymbol{v}.\nabla I\right)\nabla I\, \chi_{\Omega_m} \quad for\ H_1 \\ H'_{v}\left(\boldsymbol{v}(\boldsymbol{f}, \boldsymbol{g}), \boldsymbol{f}, \boldsymbol{g}\right) &= 2\left(\boldsymbol{v} - \boldsymbol{v}_m\right)\chi_{\Omega_m} \quad for\ H_2 \end{aligned} \tag{25}$$

where χ_{Ω_m} is the characteristic function of the set Ω_m. Equipped with the initial and adjoint fields, the gradients of the functional are simply computed from the equalities, which are none other than the partial derivative of L:

$$\begin{aligned} D_f F(\boldsymbol{f}, \boldsymbol{g}).\delta\boldsymbol{f} &= \int_{\Omega} \left(2\boldsymbol{f} + \boldsymbol{w}\right).\delta\boldsymbol{f} dV \\ D_g F(\boldsymbol{f}, \boldsymbol{g}).\delta\boldsymbol{g} &= \int_{\Omega} \left(2\nabla_t \boldsymbol{g}.\nabla_t \delta\boldsymbol{g} + \boldsymbol{w}.\delta\boldsymbol{g}\right) dV \end{aligned} \tag{26}$$

The choice of the state equation results clearly from a compromise between the simplicity of the state equation and the physics that it contributes to the problem; here, the simplest state equation has been retained (no inertial terms, no incompressibility constraint): the arbitration will be returned by the experience.

The (variational) data assimilation approach

Taking advantage of the measurements performed on a system, the general idea behind the data assimilation is to mix the information gained from the experiment, including the related uncertainties, the information gained from the modeling of the underlying physics, possibly including model uncertainties or imperfections and, lastly, *a priori* information on the system, substantially on its initial state (background information). The objective was initially to build a more precise estimation of the state, present or future, of the system. There are broadly two main families of methodologies for achieving this goal: filtering methods based on the (statistical) estimation theory [40] and variational methods [45] originally designed for meteorological forecasting applications. The general form of the functional to be minimized in data assimilation along a time interval of duration D is the following [32]:

$$J(\boldsymbol{g}, u) = \int_0^D \|H\boldsymbol{v}(\boldsymbol{g}, \boldsymbol{u}) - m\|_R^2\, dt + \int_0^D \|\boldsymbol{g}\|_F^2 dt + \int_{\Omega} \|\boldsymbol{u} - \boldsymbol{u}_0\|_B^2\, dV \tag{27}$$

where the following ingredients appear:

- v is the flow, governed by a state equation: $\partial_t \boldsymbol{v} + M(\boldsymbol{g}, \boldsymbol{u}; \boldsymbol{v}) = 0$, $\boldsymbol{v}(x,0) = \boldsymbol{v}(x)$ involving the initial state u, taken here as a control variable, and g, the perturbation of the inflow, taken as a control variable (like in Equation 18) as well;

- H is the observation operator, which maps the flow v to the measurements m, so that the first term of the functional J is simply a fidelity term to the data. The norm $\|\cdot\|_R$ used to measure the gap to the data in the data assimilation process, is built form the knowledge of measurement errors and is a covariance-based norm. In a finite dimensional setting, it reduces to the Manahobis norm generated by the inverse of the covariance matrix R: $\|x\|^2 = \langle R^{-1}x, x \rangle$.

- The second term appearing in the functional term is a regularization term on the control variable g. Again, the norm $\|\cdot\|_F$ is a covariance based norm.

- The last term involves the control variable u constituted by the initial condition of the flow, and here the regularization is related to the closeness of a background (*a priori*) information $\boldsymbol{u}_0$. The norm $\|\cdot\|_B$ is grounded in a finite dimensional setting to the covariance matrix B in the initial state.

As mentioned before, the probabilistic approach of variational data assimilation can be viewed as a regularization variational least-square identification method, but with a different reasoning behind it in the building of the regularization terms, which are based on *a priori* information (covariance matrix, backgrounds) and the peculiar feature that the regularization parameters are directly incorporated into the stabilizing functional terms via the choice of the covariance matrices. This last choice is nevertheless a delicate matter, with major concerns about cross-correlation and dependency.

In the previous example, a control variable has been added to the initial condition u, which is the only control variable in the so-called 4D-Var data assimilation method. For several years, there has been a growing demand for simultaneous identification of parameters and the estimation of state variables. Beyond the interest of exploiting large amounts of data for enhancing the simulation models (identification of model parameters) or the description of the experiments (identification of boundary conditions), a great potential can be expected either in having simulations or performing analysis for systems that do not yet exist, or even in revisiting the process of simulation itself. Joint state and parameter estimation can be simply addressed by augmenting the state variable space with the parameters $\{p\}$ and correspondingly the state equation on the parameters with the simple equation $\dot{p} = 0$ ([52], [60]). Apart from the issue of defining the related covariance operators, the adaptation of the previous formulation is straightforward. Nevertheless, this approach can be questionable on two points. First, the augmented state equation mixes quantities and equations of a very different nature, and the parameter evolution equation is somehow artificial given that the parameters are, by nature, fixed parameters. However, considered now as a function of time, it simply has to be expected that it will tend to a stationary value p^∞, in order for this value to be able to be recognized as the "true value" of the parameter. Secondly, for situations where it is impossible to have significant *a priori* statistical information about the parameters, it will be impossible to build the covariance operator and to calibrate the level of uncertainties in relation to one of the other control variables.

This is the reason why some other approaches have been proposed ([34], [3]), based on a hierarchical identification process (with a first deterministic step and a related functional energy error functional *E*), and with the choice of the covariance operator as the Hessian of *E*. As an extension of the parameter identification within a predetermined model, [1] proposed to estimate conjointly a flow and the parameters of its POD-reduced model.

Expanding, inside a body, measured surface fields

Advances in the development of digital cameras, image correlation techniques (DIC) and infrared cameras now make it possible to have measurement means for full-field surface displacements or temperatures that are cheap and relatively easy to manage and, more importantly, leading to very large amounts of information [61]; an example of estimated surface displacements on a cracked mock-up is given in Figure 3. Nevertheless, the use of these surface data is still largely restricted either to qualitative estimation or to quantitative analysis based on a plane mechanical or thermal state, or on homogeneous-through-the-thickness assumptions [12]. Aimed at a true 3D quantitative imaging process, the problem of reconstruction of the fields inside the solid from images obtained on parts of its boundary must be addressed.

One approach in dealing with this problem in mechanics is to first reformulate it within the continuous framework, taking advantage of the fact that the amount and spatial density of the information obtained using the digital image correlation techniques make it possible to consider that the complete displacement field is available on a part of the boundary and is not reduced on it to pinpoint data only. Then, it is possible secondly to formulate it as a Cauchy or Data Completion Problem, taking into account the fact that an overspecified data pair is given on a part Γ_m of the boundary: the capture of displacement fields via the DIC on a stress-free boundary with unit normal n gives access to the Dirichlet-Neumann pair $(U, \sigma.n)$. The Cauchy Problem is an archetypal ill-posed problem ([13], [33]).

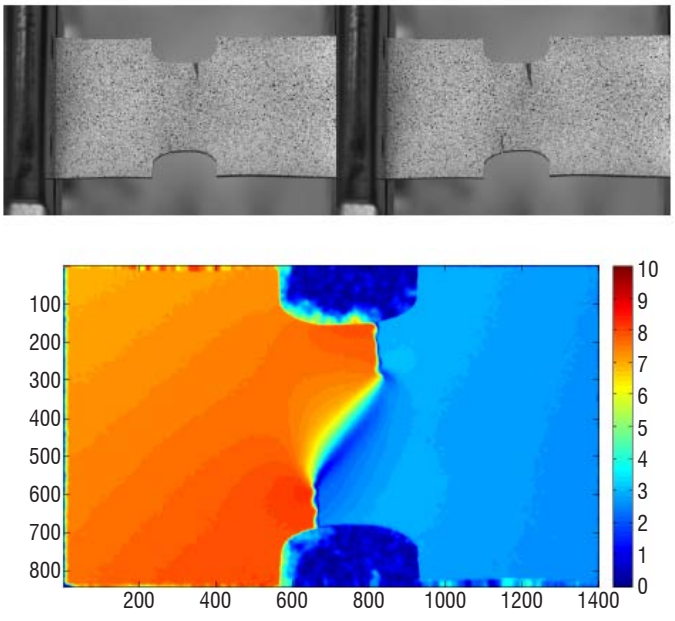

Figure 3 – Surface tangential displacement field obtained by DIC for a cracked mock-up (ONERA)

In the generic situation, the usual boundary conditions are given on Γ_b. Γ_m is the part where, using DIC acquisition measurements, both displacement and stress vector components (U_m, F_m=0) are available. Lastly, Γ_u is the remaining part of the boundary, where no boundary data is known. For the sake of simplicity, we will assume that Γ_b is empty, but the extension of the method to situations with non-empty Γ_b is straightforward. The boundary Γ_u is generally non-connected and can possibly contain internal surfaces such as cracks or boundaries of cavities and inclusions (see Figure 4).

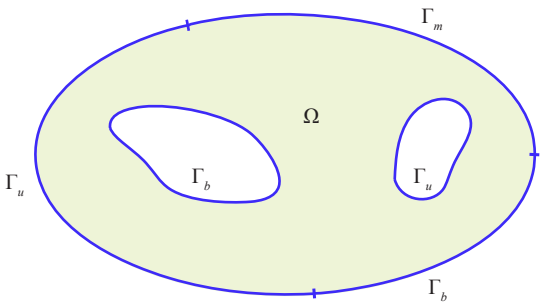

Figure 4 – The geometry of the problem with the partition (Γ_m, Γ_b, Γ_u) of the boundary of the considered body Ω

Within the framework of linearized strain and for isothermal transformation, the constitutive equation for the material constituting the solid is written in an abstract format as a relation between the Cauchy stress tensor σ and the linearized strain tensor ε, and can also involve internal variables α: $f(\boldsymbol{\sigma},\boldsymbol{\varepsilon},\alpha)=0$. This equation is complemented with the evolution equation for the internal variables α: $g(\boldsymbol{\sigma},\boldsymbol{\varepsilon},\dot{\alpha})=0$. All of these equations can also, and generally will, be inclusion equations within the framework of convex analysis, using the notion of sub-differential. The functions f and g entering the constitutive relation can be also functions of the space variable x, given that the solid Ω can be heterogeneous; however, for the sake of clarity, it will be omitted.

The form of the Data Completion Problem (or abusively the Cauchy Problem) that we can select, is to determine the missing Neumann boundary data $\eta=\sigma.n)$ on the part Γ_u of the boundary of the solid such that there exists (u, σ, α) in the domain Ω over the time interval [0, D] fulfilling the following:

$$\begin{cases} div\sigma = 0 & in\ \Omega \\ f(\boldsymbol{\sigma},\boldsymbol{\varepsilon},\alpha)=0, g(\boldsymbol{\sigma},\boldsymbol{\varepsilon},\dot{\alpha})=0 & in\ \Omega \\ \boldsymbol{u}\big|_{t=0}=\boldsymbol{u}_0\ ,\ \boldsymbol{\sigma}\big|_{t=0}=\boldsymbol{\sigma}_0\ \alpha\big|_{t=0}=\alpha_0 & in\ \Omega \\ \boldsymbol{u}\big|_{\Gamma_m}=\boldsymbol{U}_m\ ,\ \boldsymbol{\sigma}.\boldsymbol{n}\big|_{\Gamma_m}=\boldsymbol{F}_m & on\ \Gamma_m \\ \boldsymbol{\sigma}.\boldsymbol{n}\big|_{\Gamma_u}=\boldsymbol{\eta} & on\ \Gamma_u \end{cases} \quad (28)$$

where $\varepsilon(\boldsymbol{u})=\left[\nabla\boldsymbol{u}\right]^{sym}$ is the linearized strain operator. The general variational method, derived firstly in [5] for the Laplace operator (stationary isotropic conduction equation), for solving this problem is based on two steps. First, two auxiliary usual well-posed problems

Box 2 – The Bregman divergence

Introduced within the context of convex optimization ([16], [41]), the Bregman distance, or Bregman divergence, is akin to a metric, although not satisfying the triangle inequality nor symmetry. Let J be a convex function, the generalized Bregman distance between e_1 and e_2 with respect to J is the **non-negative scalar**:

$$D_J(e_1,e_2)=J(e_2)-J(e_1)-\langle p_1,e_2-e_1\rangle \quad \text{for } p_1\in\partial J(e_1)$$

where $\partial J(e)$ stands for the subdiffential of J at e.

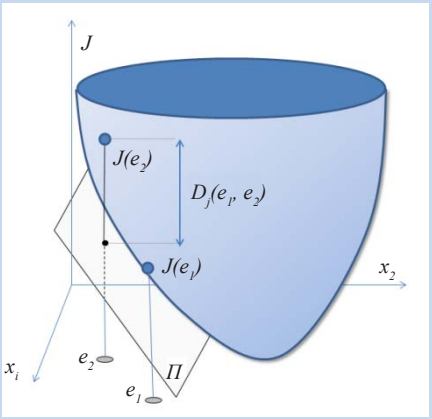

Geometrical interpretation of the Bregman divergence

Π is the tangent plane to J at e_1

In IR^n, it is readily seen that the squared Euclidean distance $\|e_1-e_2\|^2$ or Mahalanobis distance $(e_1-e_2)^T Q(e_1-e_2)$ are Bregman divergences, respectively generated by $J(x)=\|x\|^2$ and $J(x)=x^T Qx$. In probability theory, the Kullback–Leibler divergence or relative entropy [43]:

$$D(e,a)=\sum e_i \log\frac{e_i}{a_i}-e_i+a_i$$

is generated by the function

$$J(e)=\sum e_i \log e_i - e_i$$

P_i, $i = 1,2$ are defined, each using only one of the overspecified boundary data on Γ_m and a given normal stress vector field η on Γ_u:

$$\begin{cases} div\sigma_i = 0 & in\ \Omega \\ f(\boldsymbol{\sigma}_i, \boldsymbol{\varepsilon}_i, \alpha_i) = 0, g(\boldsymbol{\sigma}_i, \boldsymbol{\varepsilon}_i, \dot{\alpha}_i) = 0 & in\ \Omega \\ \boldsymbol{u}_i\big|_{t=0} = \boldsymbol{u}_0\ ,\ \boldsymbol{\sigma}_i\big|_{t=0} = \boldsymbol{\sigma}_0\ \ \alpha_i\big|_{t=0} = \alpha & in\ \Omega \\ \boldsymbol{\sigma}_i.\boldsymbol{n}\big|_{\Gamma_u} = \boldsymbol{\eta} & on\ \Gamma_u \end{cases} \tag{29}$$

And respectively for $\mathcal{P}_1$ and $\mathcal{P}_2$:

$$(\mathcal{P}_1)\{\boldsymbol{u}_1 = \boldsymbol{U}_m\ \ on\,\Gamma_m\} \qquad (\mathcal{P}_2)\{\boldsymbol{\sigma}_2.\boldsymbol{n} = \boldsymbol{F}_m\ \ on\,\Gamma_m\} \tag{30}$$

With the additional condition (global equilibrium) on $\boldsymbol{\eta}$:

$$\int_{\Gamma_m} \boldsymbol{F}_m dS + \int_{\Gamma_u} \boldsymbol{\eta} dS = 0\ .$$

It is clear that if a surface traction field $\boldsymbol{\eta}_{opt}$ on Γ_u is such that $\boldsymbol{u}_1 = \boldsymbol{u}_2 + \boldsymbol{RBM}$, where $\boldsymbol{RBM}$ is a Rigid Body Motion, the two problems $\mathcal{P}_1$ and $\mathcal{P}_2$ will have the same solution (σ, α). Therefore, the Cauchy problem is solved with $\boldsymbol{u}_1$, and the solution of the Data Completion Problem is $\boldsymbol{\eta}_{opt}$; furthermore, the Dirichlet-Neumann data pair on Γ_u is ($\boldsymbol{u}_1$, $\boldsymbol{\eta}_{opt}$).

The second step will therefore be to minimize a suitable gap functional E between the two states $(\boldsymbol{u}_1, \boldsymbol{\sigma}_1, \alpha_1)$ and $(\boldsymbol{u}_2, \boldsymbol{\sigma}_2, \alpha_2)$ solutions of $\mathcal{P}_1$ and $\mathcal{P}_2$, as a function of the sought stress vector field η on Γ_u, leading then to the variational method:

$$\boldsymbol{\eta}_{opt} = \underset{\boldsymbol{\eta}}{ArgMin}\ G(\boldsymbol{\eta}) \equiv \mathcal{E}\big([\boldsymbol{u}_1, \boldsymbol{\sigma}_1, \alpha_1](\boldsymbol{\eta}), [\boldsymbol{u}_2, \boldsymbol{\sigma}_2, \alpha_2](\boldsymbol{\eta})\big) \tag{31}$$

Clearly, the choice of the gap $\mathcal{E}$ is of primary importance, in view of the overall performance of the method. The gap functional takes into account first that the dimensions of the state variables are various, and second that the states involved are not any collections of the state variables, but rather obey a conservation law and a constitutive relation. What is needed is therefore a kind of metric defined on a geometric variety, rather than a distance in the vector space into which it is plunged.

It is therefore proposed to turn to Bregman divergences, which can be built from any convex function (see Box 2). More precisely, after having selected a convex function J of the state variables suited to each kind of constitutive relation, the gap functional is written as:

$$\mathcal{E}_J(e_1, e_2) = \int_\Omega D_J^s(e_1(x), e_2(x))dV \tag{32}$$

Where $D_J^s(e_1, e_2)$ is the symmetrized Bregman divergence:

$$\begin{aligned} D_J^s(e_1, e_2) &= D_J(e_1, e_2) + D_J(e_2, e_1) \\ &\equiv \langle p_1 - p_2, e_1 - e_2 \rangle \end{aligned} \tag{33}$$

The properties of the Bregman divergence are closely linked to the Legendre-Fenchel inequality in convex analysis ([30], [38]), especially in establishing the following property, which is of upmost importance in the perspective of building a gap functional.

Proposition: *If J is strictly convex, then the following equivalences hold true*

$$D_J^s(e_1, e_2) = 0 \Leftrightarrow e_1 = e_2 \Leftrightarrow \partial J(e_1) = \partial J(e_2) \tag{34}$$

Indeed, coming back to the solution process (13) for solving the data completion problem (10), using a gap functional based on the symmetrized Bregman divergence (33) leads to a functional correctly suited for the minimization:

$$\begin{aligned} &\mathcal{E}_J(e_1, e_2) = \int_\Omega \langle p_1 - p_2, e_1 - e_2 \rangle dV \geq 0 \\ &\mathcal{E}_J(e_1, e_2) = 0 \qquad \Leftrightarrow e_1 = e_2\ \ and\ \ p_1 = p_2 \end{aligned} \tag{35}$$

It is worth noting that the strictly convex function J does not appear anymore in the expression of the symmetrized Bregman divergence, so there is no need to compute it: it is sufficient for such a function to be able to be identified in order for the property (35) to hold true. Returning to the Data Completion Problem for extending mechanical fields inside the solid, the primal state variables are ($\varepsilon(u)$, α), and seeking convex functions J generating an appropriate and effective gap functional $\mathcal{E}_J$, one is naturally led to the convex framework of modeling for the constitutive equation. Actually, the Standard Generalized Materials [35] theory rests on the definition of a convex potential W (the free Helmholtz-Gibbs energy) and a convex pseudo-potential of dissipation Ψ (positively homogeneous of Degree 1), such that the constitutive equations appearing in (28) are written:

$$\begin{aligned} &W = W(\varepsilon - \varepsilon^p, \alpha),\ \psi = \psi(\dot{\varepsilon}^p, \dot{\alpha}) \\ &\sigma = \frac{\partial W}{\partial \varepsilon} = -\frac{\partial W}{\partial \varepsilon^p},\ A = -\frac{\partial W}{\partial \alpha} \\ &\sigma \in \partial_{\dot{\varepsilon}^p}\psi\ ,\ A \in \partial_{\dot{\alpha}}\psi \end{aligned} \tag{36}$$

Here the plastic strain ε^p appears separately in the internal variable list, and the free energy is a function of the elastic strain $\varepsilon^e = \varepsilon - \varepsilon^p$ in order to comply with the usual presentations.

For linear elasticity and non-linear elasticity (in a small strain context) where neither internal variables nor dissipation pseudo-potential are involved, the variational method (31) for solving the Data Completion Problem has been applied to the extension of surfacic displacement fields for various applications, such as identification of contact areas [6], of material parameters in inclusions, of geometry of crack fronts [7], of internal pressure in cavities [9], or determination of linear fracture mechanics parameters [8]. The following gap functional has been used:

$$G(\boldsymbol{\eta}) = \mathcal{E}_W\left(\varepsilon_1([u(\boldsymbol{\eta})]), \varepsilon_2([u(\boldsymbol{\eta})])\right) = \int_\Omega (\sigma_1 - \sigma_2) : (\varepsilon_1 - \varepsilon_2) dV \tag{37}$$

In the case of linear elasticity (quadratic potential W), the symmetrized Bregman divergence turns out to be simply twice the elastic energy of the displacement field $u_1 - u_2$: $(\sigma_1 - \sigma_2) : (\varepsilon_1 - \varepsilon_2) = 2W(\varepsilon(\boldsymbol{u}_1 - \boldsymbol{u}_2))$.

For the elastoplastic case with implicit incremental formulation [4] and taking advantage of the linearity of the Bregman divergence, that is:

$$D_{\lambda J + \mu F}(e_1, e_2) = \lambda D_J(e_1, e_2) + \mu D_F(e_1, e_2) \quad \forall \lambda, \mu \geq 0 \tag{38}$$

the following single-parameter family of gap functions can be built ($0 \leq \chi \leq 1$):

$$\begin{aligned} \mathcal{E}_{\chi W + (1-\chi)\Psi} = &\int_\Omega (\Delta\sigma_1 - \Delta\sigma_2) : \big(\chi(\Delta\varepsilon_1 - \Delta\varepsilon_2) + (1-2\chi)(\Delta\varepsilon_1^p - \Delta\varepsilon_2^p)\big) dV \\ &+ \int_\Omega \langle A_1 - A_2, (1-2\chi)(\Delta\alpha_1 - \Delta\alpha_2) \rangle dV \end{aligned} \tag{39}$$

Box 3 – Solution algorithm for the data completion problem (extension of mechanical fields for surface displacement data)

Given a Dirichlet-Neumann data pair on Γ_m: (U_m, F_m)
i) Pick an initial value η_0 of the sought stress vector on boundary Γ_u
ii) Solve the two auxiliary problems: $\mathcal{P}_1^k$ with (U_m,η_k) as boundary conditions, $\mathcal{P}_2^k$ with (F_m,η_k) as boundary conditions
iii) Compute the Gap between the two solutions of $\mathcal{P}_1$ and, $\mathcal{P}_2$: $Gk=\mathcal{E}(e_1^k,e_2^k)$
iv) If $Gk < tol$ then end, else
v) Compute the gradient of G by solving two adjoint problems
vi) Update η_k by any descent algorithm, go to ii)

The condition of strict convexity of $\chi W+(1-\chi)\Psi$ can be ensured only for $\chi>0$, because the potential Ψ is not strictly convex (as a positively homogeneous function of Degree one: $\Psi(\lambda x)=\lambda\Psi(x)$ for $\lambda\geq 0$). Within this family, the gap function obtained for $\chi=$ 1/2, which balances exactly between the free energy gap and the dissipation gap, has the peculiar feature of involving only the stress and strain tensors and can then be called the Drücker Gap:

$$\mathcal{E}_D = \int_\Omega \left(\Delta\sigma_1 - \Delta\sigma_2\right) : \left(\Delta\varepsilon_1 - \Delta\varepsilon_2\right) dV \qquad (40)$$

The Drücker Gap leads to the only computable function $G(\eta)$ by a boundary integration over the entire external boundary of the solid, as is the case in linear elasticity and hyperelasticity, using the virtual power principle. This feature has been widely used previously to improve the global performance of the solution algorithm for a linear Cauchy problem and to reduce the computational burden [6].

The following figures show the kind of results that can be achieved with respect to the extension of the mechanical field inside a solid from surface displacement measurements. The method and algorithm are summarized in Box 3. Results for linear elastic behavior were obtained with very few iterations (~ 10), whereas for strongly non-linear materials such as elastoplatic materials (elastoplaticity with linear hardening), a hundred minimizing iterations are needed.

It can be seen that either the contact surface for an elastic complex structure (Figure 5), or the residual stress after unloading for an elastoplatic solid (Figure 6) can be recovered with good accuracy.

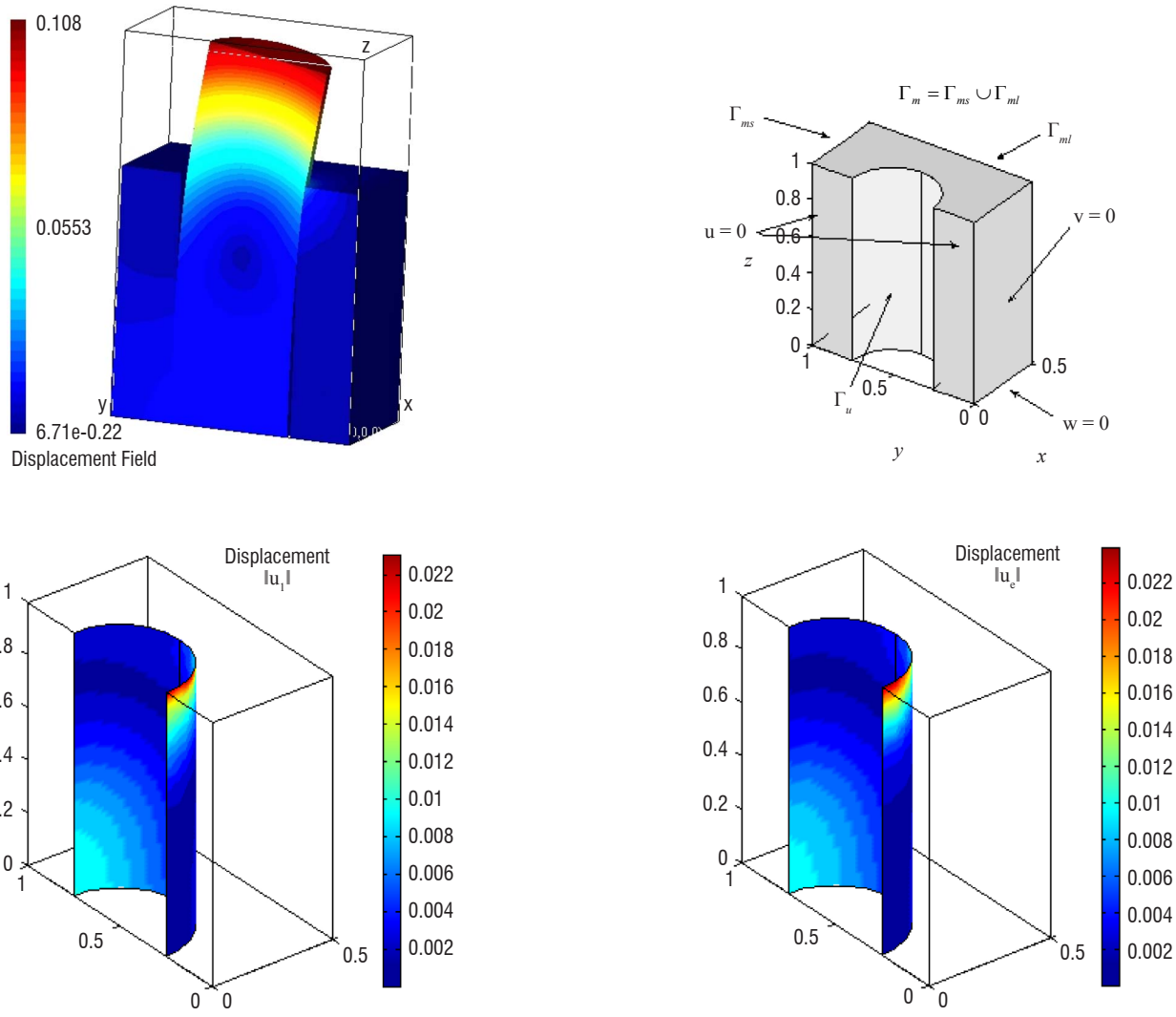

Figure 5 – 3D Identification of the displacement on the interior surface of an elastic mock-up loaded by a flexured rod (from [6])

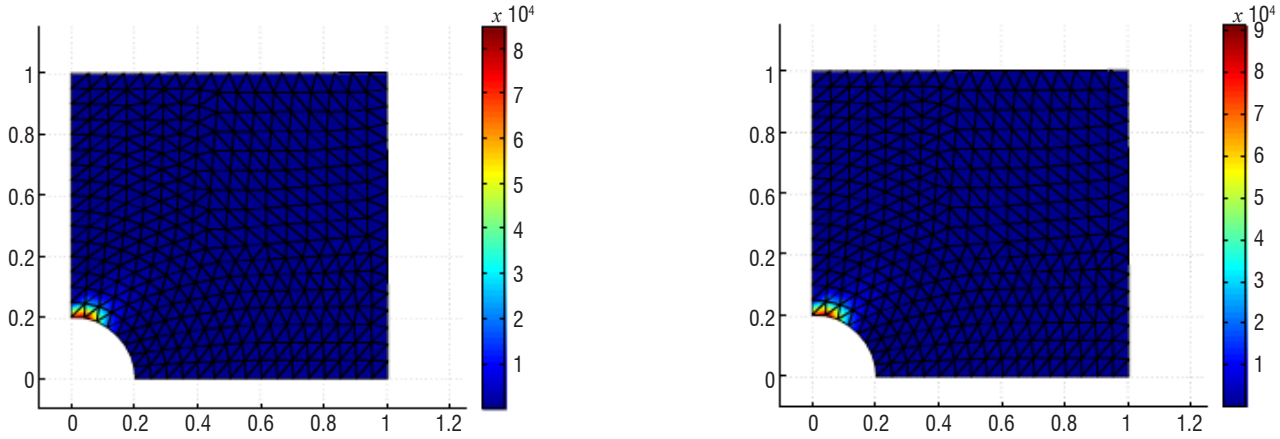

Figure 6 – Identification of residual stress (Von Mises norm) in a holed solid from a (synthetic) displacement given on the stress-free top during a loading and unloading process (from [4])

The proposed approach, using the minimization formulation (31), does not explicitly incorporate any kind of regularization, although the Cauchy problem is very ill-posed. Nevertheless, the use of a conjugate gradient algorithm entails a form of regularization in the numerical applications: the value of the stopping criterion can also plays the role of a regularization parameter [42]. For moderate noise in the data (under 2%), this regularization appears to be sufficient, as shown for the thermal conductivity equation [5].

Conclusions

This paper overviewed some results and techniques of inverse problems that can be used in signal processing on data emanating from various experimental situations arising in the aerospace domain. Two specific topics related to image-based identification problems have been focused on.

With regard to the near future, some leads or trends can be pointed out. Two promising, and already fruitful, ways can be identified in the perspective of combining measurements of distinct data acquisition nature. The first is the coupling between the 3D-PIV techniques and the 3D Background Oriented Schlieren (BOS), which is aimed at the reconstruction of the density field of instantaneous flows via the analysis of the light deflection through a medium with inhomogeneous optical index. The second is the simultaneous exploitation of the DIC displacement field measurements and the thermal camera temperature field measurements through nonlinear thermomechanics modeling. Originated by an interesting change of perspective, the passive approach to wave probing, which uses ambient noise or diffuse fields (nondestructive testing, seismic identification, echography, etc.) or non-cooperative sources of illumination (radar), stimulates a wide field of research. The deep learning applied to the analysis of a large amount of experimental data would also generate high hopes, although the number of really convincing results remains still low in the aerospace domain. From the numerical simulation side, progress can be expected thanks to the development of data assimilation, taking into account uncertainties both in the results and in the methods themselves, and enhancing performances through the use of model reduction techniques. ■

References

[1] J. D'ADAMO, N. PAPADAKIS, E. MEMIN and C. ARTANA - *Variational Assimilation of POD Low-Order Dynamical Systems*. J. Turbul, 8(9), 2007, 1-22.

[2] R. J. ADRIAN - *Particle Imaging Techniques for Experimental Fluid Mechanics.* Ann. Rev. Fluid Mechanics, 23, 1991, 261-304.

[3] S. ANDRIEUX - *Recalage, identification, suivi en service des structures.* Presses des Ponts, Paris, 2016.

[4] S. ANDRIEUX, T. N. BARANGER - *On the Determination of Missing Boundary Data for Solids with Nonlinear Material Behaviors, Using Displacement Fields Measured on a Part of their Boundaries*. J. Mech. Phys. Solids, 2016, http://dx.doi.org/10.1016/j.jmps.2016.02.008i.

[5] S. ANDRIEUX, S., T. N. BARANGER, and A. BEN ABDA - *Solving Cauchy Problems by Minimizing an Energy-Like Functional*. Inverse Problems, 22(1), 2006, 115-133.

[6] S. ANDRIEUX, S., T. N. BARANGER - *An Energy Error-Based Method for the Solution of the Cauchy Problem in 3D Linear Elasticity*. Comput. Methods Appl. Mech. Eng. 197, 2008, 902-920.

[7] S. ANDRIEUX, T. N. BARANGER - *Emerging Crack Front Identification from Tangential Surface Displacements.* C.R. Mécan. 340(8), 2012, 565-574.

[8] S. ANDRIEUX, T. N. BARANGER - *Three-Dimensional Recovery of Stress Intensity Factors and Energy Release Rates from Surface Full-field Displacements*. Int. J. Solids Struct. 50(10), 2013, 1523-1537.

[9] S. ANDRIEUX, T. N. BARANGER - *Solution of Nonlinear Cauchy Problem for Hyperelastic Solids*. Inverse Problems, 31(11), 2015, 115003-115022.

[10] R. ARCANGELI - *Pseudo-solution de l'Equation Ax=y, comptes rendus de l'Académie des Sciences. Paris, Series A*. Vol. 263A, 1966, 282-285.

[11] G. ARTANA, A. CAMMILLERI, J. CARLIER, and E. MÉMIN - *Strong and Weak Constraint Variational Assimilations for Reduced Order Fluid Flow Modeling*. Journal of Computational Physics, Volume 231, Issue 8, 20, 2012, 3264-3288.

[12] S. AVRIL, M. BONNET, A. BRETELLE, M. GRÉDIAC, F. HILD, P. IENNY, F. LATOURTE, D. LEMOSSES, A. PAGANO, E. PAGNACCO, and F. PIERRON - *Overview of Identification Methods of Mechanical Parameters Based on Full-Fields Measurements*. Exp.Mech. 48, 2008, 381-402.

[13] F. BEN BELGACEM - *Why is the Cauchy Problem Severely Ill-Posed ?* Inverse Problems 23(2), 2007, 823-836.

[14] C. BOUMAN and K. SAUER - *A Generalized Gaussian Image Model for Edge-preserving Map Estimation.* IEEE Trans. Image Processing 2, 1993, 296-310.

[15] G. E. P. BOX, J. S. HUNTER, and W. G. HUNTER - Statistics for Experimenters, John Wiley & Sons, 2005.

[16] L. BREGMAN - *The Relaxation Method of Finding the Common Point of Convex Sets and its Application to the Solution of Problems in Convex Programming*. USSR Computational Mathematics and Mathematical Physics 7 (3), 1967, 200-217. [17] J. BRYNJARSDOTTIR, and A. O'HAGAN - *Learning About Physical Parameters: The Importance of Model Discrepancy.* Inverse Problems, 30, 2014.

[18] D. CALVETTI, J. P. KAIPIO, and E. SOMMERSALO - *Inverse Problems in the Bayesian Framework.* Inverse problems, 30, 2014, Bayesien et proba.

[19] E. J. CANDÈS, and M. B. WAKIN - *An Introduction To Compressive Sampling.* IEEE Signal Processing Magazine, 21, 2008.

[20] E. J. CANDÈS, J. ROMBERG - *Sparsity and Incoherence in Compressive Sampling*, Inverse Problems, vol 23, n°3, 2007, 969-985.

[21] A. CHAMBOLLE - *An Algorithm for Total Variation Minimization and Applications.* Journal of Mathematical Imaging and Vision 20, 2004, 89-97.

[22] F. CHAMPAGNAT, A. PLYER, G. LE BESNERAIS, B. LECLAIRE, S. DAVOUST, and Y. LE SAN - *Fast and Accurate PIV Computation Using Highly Parallel Iterative Correlation Maximization*. Experiments in Fluids, 50, 2011, 1169-1182.

[23] G. CHENEGROS, L. M. MUGNIER, F. LACOMBE, and M. GLANC - *3D Deconvolution of Adaptive-Optics Corrected Retinal Images.* Proc. SPIE 6090, Three-Dimensional and Multidimensional Microscopy: Image Acquisition and Processing XIII, 60900P, February 23, 2006, DOI:10.1117/12.645233.

[24] J. M. CONAN, L. MUGNIER, T. FUSCO, V. MICHAU, and G. ROUSSET - *Myopic Deconvolution of Adaptive Optics Images by Use of Object and Point-Spread Function Power Spectra*. Applied Optics, Vol. 37, N°21, 1998.

[25] P. CORNIC, F. CHAMPAGNAT, A. CHEMINET, B. LECLAIRE, and G. LE BESNERAIS - *Fast and Efficient Particle Reconstruction on a 3D Grid Using Sparsity*. Experiments in Fluids, 56(3), 2015, 1-7.

[26] S. DAVOUST, L. JACQUIN, and B. LECLAIRE - *Dynamics of m=0 and m=1 Modes and of Streamwise Vortices in a Turbulent Axisymmetric Mixing Layer.* J. Fluid Mech. Vol. 709, 2012, 408-444.

[27] G. DESODT, L. AOUCHICHE, and O. RABASTE - *Extract Before Detect, N-Signal Complex Approximate Message Passing Applied to Radar Signals*. COSERA (COmpressed SEnsing Applied to RAdar Signals), Bonn, 2013.

[28] D. L. DONOHO - *Compressed Sensing.* IEEE Trans. IT, vol. 52/no. 4, 2005, 1289-1306.

[29] D. L. DOHONO, and X. HUO - *Uncertainity Principles and Ideal Atomic Decomposition.* IEEE Trans. Inform.Theory, Vol. 47, n°7, 2001, 2845-2862.

[30] I. EKELAND, and R. TÉMAM - *Convex Analysis and Variational Problems*, Siam, Philadephia, 1999.

[31] D. P. G. FOURES, N. DOVETTA, D. SIPP, and P. J. SCHMID - *A Data-Assimilation Method for Reynolds-Averaged Navier-Stokes-Driven Mean Flow Reconstruction.* J. Fluid Mech., 759, 2014, 404-431.

[32] A. GRONSKIS, D. HEITZ, and E. MÉMIN - *Inflow and Initial Conditions for Direct Numerical Simulation Based on Adjoint Data Assimilation.* Journal of Computational Physics ,242, 2013, 480-497.

[33] J. HADAMARD - *Lectures on Cauchy's Problem in Linear Partial Differential Equations*. Dover, NewYork, 1923.

[34] K. HADJ-SASSI, and S. ANDRIEUX - *Vers une nouvelle stratégie d'estimation conjointe des paramètres matériaux et de l'état des structures par assimilation de données et recalage.* 18ème Congrès Français de Mécanique, Grenoble, 2007.

[35] B. HALPHEN, and Q. S. NGUYEN - *Sur les matériaux standards généralisés*. J. Mécanique, 14, 1975, 39-63.

[36] P. HEITZ, D. HEITZ, and E. MÉMIN - *Multiscale Regularization Based on Turbulent Kinetic Energy Decay for PIV Estimation with High Spatial Regularization.* 8th Int. symposium on particle image velocimetry-PIV 2009, Melbourne, Victoria, Australia, 2009.

[37] D. HEITZ, E. MÉMIN, and C. SCHNÖRR - *Variational Fluid Flow Measurements from Image Sequences: Synopsis and Perspectives*. Exp. Fluids, 48, 2010, 369-393.

[38] J.-B. HIRIART-URRUTY, and C. LEMARÉCHAL - Convex Analysis and Minimization Algorithms, I and II. Springer Verlag, 1993.

[39] J. KAIPIO, and E. SOMERSALO - *Statistical Inverse Problems: Discretization, Model Reduction and Inverse Crimes.* J. Computational and Applied Mathematics, 198, 2007, 493-504.

[40] R. E. KALMAN - *A New Approach to Linear Filtering and Prediction Problems.* Transactions of the ASME - Journal of Basic Engineering (Series D), 1960, 82: 35-45.

[41] K. C. KIWIEL - *Proximal Minimization Methods with Generalized Bregman Functions*. SIAM J. Control Optim. 35 (4), 1997, 1142-1168.

[42] M. Y. KOKURIN - *Stable Iteratively Regularized Gradient Method for Nonlinear Irregular Equations Under Large Noise.* Inverse Problems 22, 2006, 197-207.

[43] S. KULLBACK, and R. A. LEIBLER - *On Information and Sufficiency*. Annals of Mathematical Statistics 22 (1), 1951, 79-86.

[44] M. M. LAVRENTIEV - Some Improperly Posed Problems of Mathematical Physics. Springer, Berlin, 1967.

[45] F. X. LE DIMET, and O. TALAGRAND - *Variational Algorithms for Analysis and Assimilation of Meteorological Observations: Theoretical Aspects.* Tellus, 38A, 1986, 97-110.

[46] J. L LIONS - Optimal Control of Systems Governed by Partial Differential Equations. Springer Verlag, 1971.

[47] A. MOHAMAD-JAFARI, and M. DUMITRU - *Bayesian Sparse Solution to Linear Inverse Problems with Non Stationary Noise With Student-t Priors.* Digital Signal Processing, Special Issue on Bayesian Signal Processing: in Honour of William J. Fitzgerald, 2015.

[48] J. MORLIER, and D. BETTEBGHOR - *Compressed Sensing Applied to Modeshapes Reconstruction.* in Topics in Modal Analysis I, Volume 5, Part of the series Conference Proceedings of the Society for Experimental Mechanics Series,2012, 1-8.

[50] V. A. MOROZOV - *On the solution of functional equations by the method of regularization*. Soviet Math. Dokl. 7, 1966, 414-417.

[51] L. MUGNIER, T. FUSCO, J.-M. CONAN - *MISTRAL: a Myopic Edge-Preserving Image Restoration Method, with Application to Astronomical Adaptive-Optics-Corrected Long-Exposure Images.* J. Opt. Soc. Am. A, 21, 2004, 1841-1854.

[52] I. M. NAVON - *Practical and Theoretical Aspects of Adjoint Parameter Estimation and Identifiability in Meteorology and Oceanography.* Dynamics of Atmosphere and Oceans, 27, 1997, 55-79.

[53] D. L. PHILLIPS - *A Technique for the Numerical Solution of Certain Integral Equations of the Ffirst Kind.* J Assoc Comput Mach, 9, 1962, 84-97.

[54] L. I. RUDIN, S. OSHER, and E. FATEMI - *Nonlinear Total Variation Based Noise Removal Algorithms*. Physica D 60, 1992, 259-268.

[55] P. RUHNAU, and C. SCHNÖRR - *Optical Stokes Flow Estimation: An Imaging-Based Control Approach*. Exp. Fluids, 2007, 42: 61-78.

[56] P. RUHNAU, A. STAHL, and C. SCHNÖRR - *On-line Variational Estimation of Dynamical Fluid Flows with Physics-Based Spatio-Temporal Regularization.* In Pattern Recognition – 28th DAGM Symposium, volume 4174 of LNCS, Springer, 2006, 444-454.

[57] P. RUHNAU, A. STAHL, and C. SCHNÖRR - *Variational Estimation of Experimental Fluid Flows with Physics-Based Spatio-Temporal Regularization*. Measurement Science and Technology, 2007, 18: 755-763.

[58] F. SARTOR, G. LOSFELD, and R. BUR - *PIV Study on a Shock-Induced Separation in a Sransonic Flow.* Exp. Fluids Vol. 53, 2012, 815-827.

[59] C. SCHNÖRR - *Determining Optical flow for Irregular Domains by Minimizing Quadratic Functionals of a Certain Class.* Int. J. Computer vision, 6:1, 1991, 23-35.

[60] P. SMITH, S. L. DANCE, M. J. BAINES, N. K. NICHOLS, and T. R. SCOTT - *Variational Data Assimilation for Parameter Estimation: Application to a Simple Morphodynamic Model.* Ocean Dynamics, 59 (5), 2009, 697-708.

[61] A. SUTTON, and J. H. S. ORTEU - Image Correlation for Shape, Motion and Deformation Measurements: Basic Concepts, Theory and Applications. Springer, USA, 2009.

[62] R. TIBSHIRANI - *Regression Shrinkage and Selection via the Lasso.* J. of the R. Stat. Soc, Series B, Vol. 58, 1 , 1996.

[63] A. N. TIKHONOV and V. Y. ARSENIN - Solutions of Ill-Posed Problems. Wiley, New York, 1977.

[64] E. ROSENCHER - *Optical Diagnostics of Flows: an Introduction.* AerospaceLab Journal, 1, 2009, 1-2.

[65] G. VASILE, J. P. OVARLEZ, F. PASCAL, and C. TISON - *Coherency Matrix Estimation of Heterogeneous Clutter in High-Resolution Polarimetric SAR Images, Geoscience and Remote Sensing.* IEEE Transactions on 48 (4), 2010, 1809-1826.

[66] A. VLASENKO, and C. SCHNÖRR - *Physically Consistent Variational Denoising of Image Fluid Flow Estimates.* IEEE Trans Image Process,19(3), 2010, 586-952.

[67] M. J. WAINWRIGHT - *Sharp Thresholds for High-dimensional and Noisy Sparsity Recovery Using I1-Constrained Cuadratic Programming (Lasso).* IEEE Trans.IT, v.55, no. 5, 2009.

[68] R. YEGAVIAN, B. LECLAIRE, F. CHAMPAGNAT, and O. MARGUET - *Performance Assessment of PIV Super-Resolution with Adjoint-Based Data Assimilation.* 11th Int. Symposium on Particle image velocimetry – PIV15, Santa Barbara, California, Sep 14-16, 2015.

AUTHOR

Stéphane ANDRIEUX received his Engineering diploma from the *Ecole Nationale des Ponts et Chaussées*, France, in 1980, and later his PhD in 1983. He joined the R&D division of *Electricité de France* in 1985 and led various research groups and mechanics departments there. After being the Scientific Director of the EDF R&D division, he is now the General Scientific Director of ONERA and professor at *Ecole des Ponts Paristech*. His work is focused on damage mechanics and inverse problems. In 2006, he received the Dechelle Prize from the French Academy of Sciences.